Heliyon 9 (2023) e21219

Contents lists available at ScienceDirect

Heliyon

journal homepage: www.cell.com/heliyon

Network pharmacology and in vivo and in vitro experiments to determine the mechanism behind the effects of Jiawei Yanghe decoction via TLR4/Myd88/NF-κB against mastitis

Jing Zhao [a,1], Liuyan Xu [a,1], Lingyan Lv [a], Liuyi Wang [f], Xuan Wang [a], Chen Liang [d], Chunhui Wang [e], Yan Qiu [c,**], Xiaohua Pei [b,*]

[a] Beijing University of Chinese Medicine Third Affiliated Hospital, Beijing, 100029, China
[b] Xiamen Hospital of Beijing University of Traditional Chinese Medicine, Xiamen, 361015, China
[c] Eye Institute of Xiamen University, Xiamen, 361102, China
[d] Dongfang Hospital Beijing University of Chinese Medicine, Beijing, 100078, China
[e] Fangshan Hospital Beijing University of Chinese Medicine, Beijing, 102488, China
[f] Xiamen University, Xiamen, 361102, China

ARTICLE INFO

Keywords:
Lactation mastitis
Jiawei Yanghe decoction
Network pharmacology
Molecular docking
LPS
TLR4/Myd88/NF-κB

ABSTRACT

Background: In the Qing dynasty, Yanghe decoction was as a therapeutic soup for effectively treating chronic inflammatory disorders. It was used as a therapeutic soup for effectively treating chronic inflammatory disorders. In the clinical use of Yanghe decoction, the adjustment of the medication for a variety of inflammatory diseases have therapeutic effect, including mastitis. Therefore, Jiawei Yanghe decoction (JWYHD) may be used to treat inflammatory breast diseases.
Methods: First, LM- and JWYHD-related components were retrieved from the database and analysis platform. Next, protein–protein interaction networks were constructed to screen the key targets, and gene ontology and Kyoto encyclopedia of gene and genome enrichment analyses were performed to predict the potential biological functions and mechanisms of JWYHD. Simultaneously, the JWYHD samples were collected and analyzed by UPLC–HRMS. Finally, in vivo and in vitro experiments were conducted to construct animal and cellular inflammation models of mastitis with LPS. Pathological changes in the mammary tissues were detected. Enzyme-linked immunosorbent assay, reverse transcription-polymerase chain reaction, and Western blotting was performed to determine the mRNA and protein levels of inflammatory cytokines and toll-like receptor 4/myeloid differentiation primary response 88/nuclear factor kappa B signaling pathway in the breast tissues to elucidate the potential underlying mechanisms of anti-mastitis effects of JWYHD from different aspects.
Results: In total, 103 compounds were detected in JWYHD by UPLC–HRMS. 691 active ingredients of JWYHD were screened by network pharmacology, and 47 LM-related targets were identified. The PPI network analysis of the targets revealed the 5 core targets. The KEGG enrichment results established the NF-κB signaling pathways as the core. After JWYHD intervention, low

* Corresponding author.
** Corresponding author.
E-mail addresses: pisces0226@bucm.edu.cn (J. Zhao), xuliuyan0421@163.com (L. Xu), lly2090@126.com (L. Lv), 546375839@qq.com (L. Wang), 1508123446@qq.com (X. Wang), 150474380@qq.com (C. Liang), ghostrip@163.com (C. Wang), yanqiu@xmu.edu.cn (Y. Qiu), pxh_127@163.com (X. Pei).
[1] J. Zhao and L. Xu are the co-first author.

https://doi.org/10.1016/j.heliyon.2023.e21219
Received 5 July 2023; Received in revised form 15 September 2023; Accepted 18 October 2023
Available online 21 October 2023

inflammatory enrichment and mild inflammatory damage in breast tissues were observed. Furthermore, JWYHD treatment affected mammary gland inflammatory cytokines and the TLR4/Myd88/NF-κB signaling pathway by considerably reducing the respective protein levels and gene expression; thus, JWYHD alleviated LM symptoms.

Conclusions: We hypothesized and demonstrated the anti-inflammatory effects of JWYHD by cytokine regulation via the TLR4/Myd88/NF-κB signaling pathway. In conclusion, JWYHD showed its potential in LM treatment and in treating other acute and chronic inflammatory diseases.

Abbreviations

JWYHD	Jiawei Yanghe Decoction
LM	Lactation mastitis
TCM	Traditional Chinese Medicine
GO	Gene Ontology
KEEG	Kyoto Encyclopedia of Genes and Genomes
PPI	Protein–protein interaction
TCMSP	TCM systems pharmacology Database and analysis Platform
Uniprot	Universal protein
LPS	Lipopolysaccharide
MPO	Myeloperoxidase
NF-κB	Nuclear factor-κappa B signaling pathway
MS	Mass spectrometric
OMIM	Online Mendelian Inheritance in Man
OB	Oral bioavailability
DL	Drug-likeness
BUCM	Beijing University of Chinese Medicine
BP	Biological process
CC	Cellular component
MF	Molecular function
HE	Hematoxylin and Eosin
UPLC-HRMS	Ultra Performance Liquid Chromatography - High-Resolution Mass Spectrometry
DEX	Dexamethasone
PBS	Phosphate-buffered saline
TP53	Tumor protein 53
PTGS2	Prostaglandin G/H synthase 2

1. Introduction

Also known as acute mastitis, lactation mastitis (LM), is a disease that affects approximately 33 % of postpartum women about six weeks after delivery [1]. Early local LM symptoms include redness, swelling, heat, pain, and decreased breast milk production, with or without systemic symptoms, such as fever, chills, and headache [2], as well as varying degrees of nipple cracking and milk clotting. Moreover, if the inflammation is not promptly controlled and treated, 11 % of patients develop breast abscesses [3,4]. LM harms the health and quality of life of breastfeeding mothers and infants, by creating burdens of disease and exposing them to risks of life-threatening conditions [5]. Moreover, some 10 % of LM patients discontinue breastfeeding [6], making it one of the most significant barriers to increasing breastfeeding rates [7,8].

The development of breast inflammation is a standard and complex process. In postpartum women, bacteria can access mammary glands retrogradely through the nipple tubes, inducing the production of inflammatory cytokines by typical immune and inflammatory cells, such as interleukin (IL)-1, IL-6, and tumour necrosis factor (TNF)-α [9–12]. Antibiotic therapy is a preferred treatment for alleviating breast inflammation symptoms [2,8]. However, continuous antibiotic use can induce bacterial resistance, increase the risk of infection and severely disrupt the homeostasis of the human microbiota [13–16]. In addition, the widespread use of antibiotics can severely disrupt the ecological stability and species diversity of normal human microflora [17]. Studies have investigated the effects of ciprofloxacin on the intestinal microflora of three healthy individuals via sequencing; results suggested that the diversity of the microflora in the subjects was reduced and did not recover even after six to ten months of discontinuing the antibiotics. In addition, low-abundance flora became completely extinct [18,19]. Thus, the need for alternative therapeutic approaches for treating breast inflammation is indicated. Herbs from traditional Chinese medicine (TCM), both in formulations and as a single active ingredient, have

shown low resistance to the dual regulation of a bacterium and a host by altering the permeability of biological membranes and ion channels and inhibiting bacterial enzyme activities [20–22]. For a more effective and early prevention and treatment of LM and to reduce its incidence and the progression of breast abscesses, the use of herbal medicines from TCM can be a potential treatment approach [23,24].

A Yanghe decoction, of seven herbs, namely *Rehmannia glutinosa* (Gaertn.) DC.(RGD),*Cervus.elaphus Linnaeus*(CEL),Zingiber

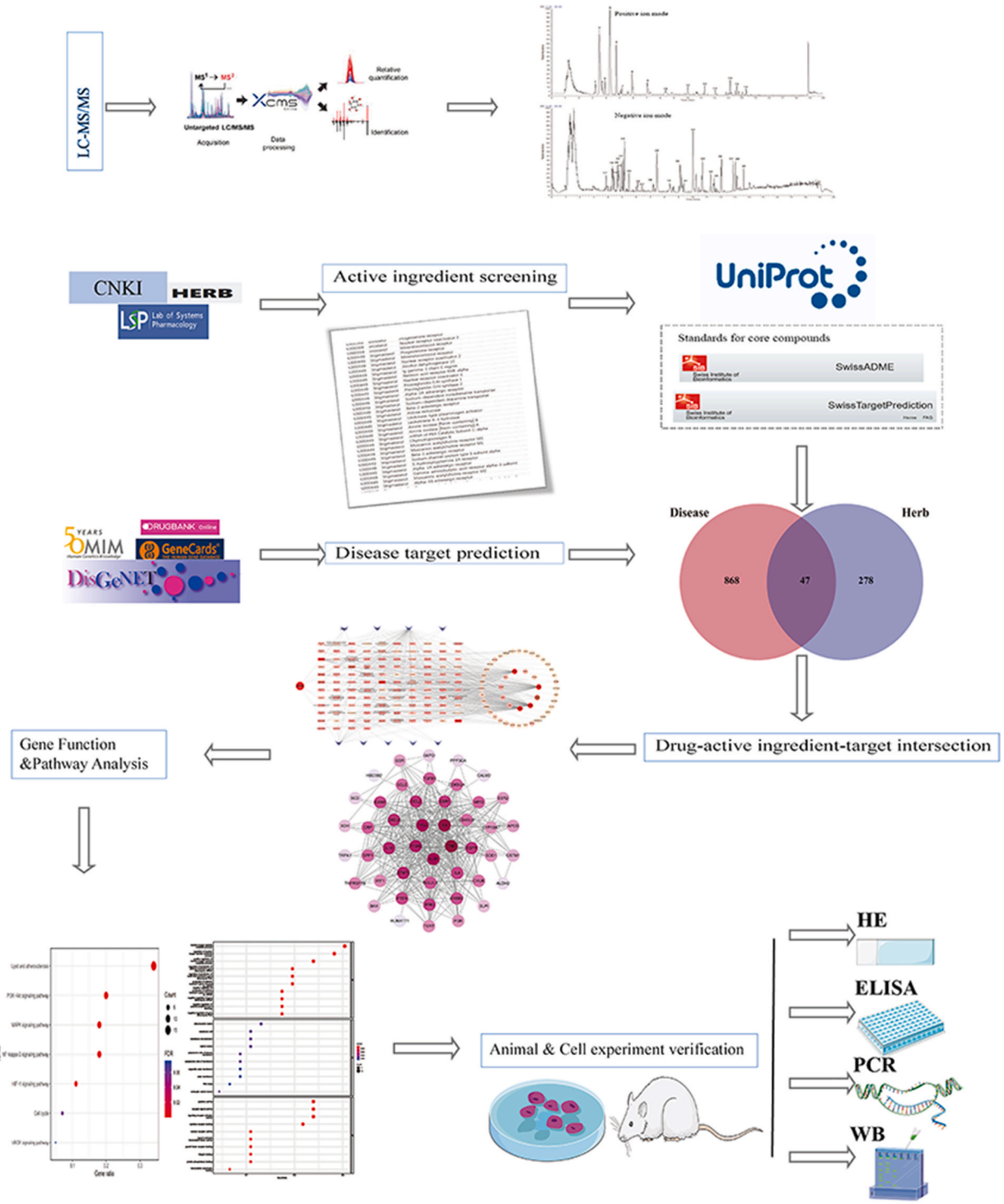

Fig. 1. Depiction of a network pharmacology-based approach to comprehend JWYHD's chemical mode of action against LM.

officinale Roscoe(ZOR), *Cinnamomum cassia* (L.) D. Don.(CCD), *Ephedra sinica* Stapf (ESS),*Sinapis alba* L.(SA) and *Glycyrrhiza uralensis* Fisch.(GUF), was first mentioned in Hongxu Wang's "*The Complete Collection of Surgical Evidence and Treatment*"in the Qing Dynasty [25]. Studies have reported the frequent use of the Yanghe decoction, with or without other compounds, in clinical practice to treat inflammatory diseases, such as immune thyroid disease, osteoporosis, and pulmonary asthma, by reducing inflammation and regulating immunity [26–28]. In addition, the prior clinical use of the Yanghe decoction, with or without other compounds, for in treating LM, reduced inflammatory factors, including TNF-α and considerably alleviated disease symptoms [29]. Nonetheless, there is a need for a clear explanation of the underlying mechanism of action of the Yanghe decoction. *Gypsophila vaccaria (L.) Sm.*(GVS) and *Leonurus japonicus Houtt.*(LJH) have been added to a Jiawei Yanghe decoction (JWYHD) to increase tits efficacy in postpartum women considering their physiological characteristics, which are characterised by "many deficiencies and stasis" during this period.(The plant name has been checked by MPNS and the medicinal animal ingredient has remained consistent in common use). This study used ultra-performance liquid chromatography–high-resolution mass spectrometry (UPLC-HRMS) to analyze, the chemical composition of JWYHD. Then, network pharmacology was combined with molecular docking to validate the network pharmacology predictions regarding the targets and potentially significant pathways of JWYHD against LM. Based on in vivo and invitro experiments in the animal and cells, we further validated the effects of JWYHD on lipopolysaccharide (LPS)-induced LM were validated. The results of this study provide experimental data promoting the continued development and clinical use of JWYHD, as well as an experimental basis for the study of the role of Chinese anti-inflammatory medicine in treating related diseases. Fig. 1 illustrates the research methodology.

2. Materials and methods

2.1. Identification of the main chemical components by UPLC-HRMS

For the identification, approximately 1.0 g of JWYHD sample was taken in a 15-mL centrifuge tube, treated with 10 mL of 70 % methanol aqueous solution, vortexed, sonicated for 90 min, and centrifuged at 16000×*g* for 15 min at 4 °C. Then, 1.0 mL of the supernatant was freeze-dried under vacuum, and 2 mL of a 40 % methanol aqueous solution was added to the sample residue after lyophilization, vortexing, and centrifuging at 16000×*g* for 15 min at 4 °C. For UPLC-HRMS analysis, the supernatant was extracted.

Chromatography conditions: the extracts of YQHX were analyzed by using the Vanquish UHPLC system (Thermo Scientific, Waltham, MA) fitted with an HSS-T3 column (100 × 2.1 mm, 1.8-μm particle size, Waters) at a column compartment temperature of 35 °C. Mobile phase A was composed of H_2O + 0.1 % formic acid; mobile phase B was composed of acetonitrile +0.1 % formic acid (LC-MS grade solvents, Fisher Chemical). The samples were separated using the following gradient at the flow rate of 0.3 mL/min: 1 min isocratic at 5 % B, 98 % B in 16 min, 5 % B in 0.5 min, and 2.5 min isocratic at 5 % B.

Mass spectrometry conditions: The UHPLC system was coupled with the Q-Exactive HFX Mass Spectrometer (Thermo Fisher Scientific, Bremen, Germany). Mass spectra were acquired in the positive and negative electrospray ionization modes (ESI) using data-dependent acquisition (DDA) mode with a mass range of 90–130 *m/z*. The MS/MS spectra were generated using the 10 most-intense MS1 ions. The stepped normalized high-energy dissociation (HCD) collision energies (CEs) of 20, 40, and 60 units were utilized. The capillary temperature was set to 320 °C, while the temperature of the probe heater was set to 370 °C.

2.2. Active ingredient screening

The chemical composition of JWYHD was determined using the TCMSP database (https://tcmsp-e.com/) [30] and the HERB database (http://herb.ac.cn/) in conjunction with a literature search. The composed chemical compositions were individually run through the Pubchem database (https://pubchem.ncbi.nlm.nih.gov/) to obtain molecular structure maps of the components, which were then saved in the 3Dsdf format. The structures of the obtained compounds were uploaded to the Swiss ADME platform (http://www.swissadme.ch/). The criteria for setting the potential core compounds were as follows: (1) gastrointestinal absorption (GIabsortion) of "High," indicating a good oral bioavailability and absorption of the ingredient; (2) setting 5 categories of pharmacophore prediction (Lipinski, Ghose, Veber, Egan, and Muegge) with two or more "Yes" results. The target proteins with a probability ≥0.5 were screened as possible targets for drug action using Swiss Target Prediction (http://www.swisstargetprediction.ch/).

2.3. Disease molecular-target prediction

The data were collected from the OMIM (https://omim.org/), GeneCards (https://www.genecards.org/), DrugBank (https://go.drugbank.com/), and Disgenet (https://www.disgenet.org/) databases [31] using the subject terms "Acute Mastitis" or "Lactation Mastitis" and the species "Homo" to ensure accuracy and completeness. The DrugBank database is based on clinical trial drug evidence and provides abundant drug data and comprehensive drug target information, whereas the OMIM, Gene Cards, and Disgenet databases are based on literature; each database has certain benefits and complements the others. The targets were combined after removing the duplicate values obtained from the abovementioned databases. The known targets of the unanticipated active ingredients were added based on the reports of scientific literature. The UniProt protein database (https://www.uniprot.org) was used to assign a gene symbol to the potential targets of disease targets and drug components. The two were then subsequently mapped to obtain the potential targets for intervention in mastitis in JWYHD.

2.4. Major components, target intersections, and network construction

The *E* Venn (http://www.ehbio.com/test/venn/#/) website [32] mapped the two by combining the active ingredients of TCM with the disease targets obtained from the database so as to determine the average scores of both. STRING, a database of protein interactions, was used to conduct bioinformatic analysis, while Cytoscape 3.8.0 was used to construct a protein–protein interaction (PPI) network of target drug molecule-disease targets.

2.5. GO functional and KEGG pathway enrichment analysis

The bioinformatics database DAVID 6.8 (https://david.ncifcrf.gov/) was used to analyze the disease-target drug molecules and the disease-common potential targets. Similarly, information was extracted utilizing the R language 3.6.2 program based on data packages such as Bioconductor, with $P < 0.05$ considered as the threshold. The GO and KEGG enrichment analysis histogram and the bubble plot were generated. $P < 0.01$ was considered to indicate statistical significance.

2.6. Molecular docking analysis

A molecular docking technique was used to dock the active ingredients with high median network relationship values using action-related potential targets to score the predicted ability of JWYHD active ingredients to intervene in LM. The 3D structure information of JWYHD components was obtained from the TCMSP database and PubChem database, while the 3D crystal structure of the target proteins was downloaded from the RCSB database (http://www.rcsb.org/pdb) and saved in the pdb format; the Surflex-dock module in SYBYL-X 2.1.1 software was used for molecular docking.

2.7. Animals and grouping

Pregnant BALB/c mice (body weight: 20–28 g) were obtained from the Beijing Viton Lever Laboratory Animal Co. Each cage contained a single animal. All animals were provided access to free water and laboratory rodent food in a clean laboratory (at 22–25 °C under 50–70 % relative humidity). Seven days were allocated for acclimation rearing and observation of pup production. All animal experiments were conducted in accordance with the US National Institutes of Health's Guide for the Care and Use of Laboratory Animals, as approved by the Animal Ethics Committee of Xiamen University (XMULAC20200055).

2.8. Sample preparation

All herbs used in this study were commercially available in dried form and purchased from the herbal pharmacy of Xiamen Hospital of Beijing University of Traditional Chinese Medicine and identified by the hospital's pharmacy department physicians. JWYHD consists of 9 herbs (84 g/dose) in the following prescription ratios: RGD:CEL:ZOR:CCL:ESS:SA: GVS:LJH:GUF at 5:3:4:1:1:1:3:5:5. The dosages of the herbs in JWYHD are based on the principles of traditional Chinese medicine. The herbs, excluding the antler gum mixture, were soaked for 0.5–1 h in 1500 mL of water. The resulting decoction was cooked on a military fire for 30 min and then switched to a civilian fire, with continued cooking for an additional 1 h. After filtering the liquid through multiple layers of gauze, water was added to the decoction. In order to obtain the JWYHD aqueous decoction, the liquid solutions from both decoctions were combined, to which antler gum was added and dissolved. The resultant liquid was then concentrated into a paste form using an evaporator under reduced pressure and placed in a refrigerator at −20 °C for freezing. After condensation, the JWYHD preparation was placed in a freeze dryer for low-temperature sublimation and evaporation.

2.9. Reagents and apparatus

OriCell® Premium Fetal Bovine Serum (FBSSR-01021-500, Saiye); RPMI-1640 medium (SH30809.01, Gibco); Penicillin-Streptomycin (15140122, Gibco); phosphate-buffered saline 1 × (SH30256.01,HyClone); Cell Counting Kit-8 (SD6212, Simuwubio Co., Ltd, Shanghai, China). LPS was obtained from Sigma-Aldrich (lot number: L2880-10 MG). Dexamethasone (DEX) injections were acquired from Xiamen Hospital of Traditional Chinese Medicine (production lot number: 220304187, Zhengzhou Zhoufeng Pharmaceutical Co., Ltd.). The protein assay kit (TNF-α, IL-6, IL-1β, and MPO) was obtained from Simuwubio Co., Ltd. The reverse transcription kit was obtained from TAKARA (Japan). All other chemicals were of reagent grade. Rabbit CD177 was obtained from Cell Signaling Technology (1:100, Danvers, Massachusetts, USA). Mouse anti-TLR4 was bought from Santa Cruz Biotechnology (1:800, Dallas, Texas, USA). Rabbit anti-p65 was obtained from Cell Signaling Technology (1:1000, Danvers), and rabbit anti-IκB was obtained from Abcam (1:5000, USA). Rabbit antibodies against β-actin, horseradish peroxidase (HRP)-conjugated goat anti-mouse, and anti-rabbit IgG antibodies were bought from Simuwubio Co., Ltd.

2.10. Grouping and experimentation

The offspring were separated for 3 h before modeling, and the mice were anesthetized and then placed under a dissecting microscope. The fourth pair of teats and their surroundings were disinfected with 75 % ethanol, and the teats were cut with sterile scissors to a length of 1 mm. Subsequently, 50 μL of LPS (0.2 mg/mL) was injected into the mice's mammary ducts with a 32G micro-needle.

The mice were randomly assigned to the blank group, the LPS group, the LPS + JWYHD low-dose group 0.2 mL (0.6825 g/kg), the LPS + JWYHD medium-dose group 0.2 mL (1.365 g/kg), the LPS + JWYHD high-dose group 0.2 mL (2.73 g/kg), and the LPS + DEX group (5 mg/kg). The JWYHD-intervention group received varying doses of JWYHD via gavage, beginning approximately 5–7 days after delivery for 6 days, once a day. In the DEX group, 0.2 mL DEX solution (0.5 mg/kg) was intraperitoneally administered 1 h before and 12 h after modeling. The serum and mammary tissues were collected 24 h after LPS injection and stored at −80 °C for subsequent analysis.

2.11. Cell culture and treatment

HC11 mammary epithelial cells were used as experimental subjects. In the lipopolysaccharide-induced inflammation model, a final concentration of 1 μg/mL of lipopolysaccharide was selected to induce an inflammatory response [33–35]. The cultured mammary epithelial cells were assigned to the following five groups: blank control group, LPS group, LPS + JWYHD group (1,1.5, and 2 mg/mL). The LPS + JWYHD group was given JWYHD (1,1.5, and 2 mg/mL) pretreatment followed by LPS for 24 h, and the blank control group was administered the same volume of cell culture solution.

2.12. Cell viability assay

The CCK-8 assay (SD6212, Simuwubio Co., Ltd.) was performeddetect cell viability. The experimental cells were inoculated into a 96-well plate for 24 h, and treated with JWYHD (1,1.5, and 2 mg/mL)for 24 h, after which 10 μL of the CCK-8 solution was added to each well for 2 h. The absorbance at 450 nm was detected using an enzyme marker. The cell survival rate was calculated using the absorbance OD value, and the experiment was repeated thrice.

2.13. Histopathological examination and immunohistochemistry

The female mice's mammary glands were removed, fixed in a 4 % formaldehyde solution, and then cut into sections in line with a predetermined process. The pathological changes in the mammary glands of all groups were evaluated. A random histological evaluation was conducted using a scoring system, as described elsewhere [36]. Briefly, the slices of pathological tissue were assessed by three expert researchers. According to the neutrophil aggregation, bleeding, acinar integrity, and changes in the acinar wall thickness, each segment was split into 5 visual areas. The scores were graded as follows: 0 = no injury, 1 = a minor injury, 2 = a moderate injury, 3 = a serious injury, and 4 = an exceedingly severe injury.

The standard immunohistochemical processes were followed. Briefly, the segments were sequentially baked, dewaxed in xylene, and hydrated in a gradient series of alcohol. Then, endogenous peroxidase was eliminated from the sections using 3 % H_2O_2. Before to incubation with specific primary antibodies, such as CD177, the immunostained slices were pre-incubated with 5 % normal goat serum (1:1000, Danvers). Dako's horseradish peroxidase streptavidin-biotinylated secondary antibody was used to prepare the sections, followed by the addition of diaminobenzidine (DAB kit, Vector Laboratories). For the negative controls, non-immune rabbit or mouse serum was used *in lieu* of the main antibody. By measuring the integrated optical density (IOD) with a light microscope and a computer-based ImageJ Morphometric System, the staining levels were ascertained.

2.14. Enzyme-linked immunosorbent assay (ELISA)

The manufacturer's guidance was followed when using the ELISA kit to determine the levels of inflamed proteins TNF-α, IL-1β, IL-6, and MPO. Briefly, the mammary gland tissues were collected 24 h after LPS stimulation. The samples were weighed and homogenized at a 1:9 w/v ratio with PBS. The supernatant was centrifuged and collected to analyze the levels of TNF-α, IL-1β, IL-6, and MPO.

2.15. Reverse transcription-polymerase chain reaction (RT-PCR)

The RNA was extracted with Trizol. After the samples were treated with a gDNA wipe combination, RNA was reverse-transcribed into cDNA for qPCR using the TAKARA PrimeScript™ RT reagent kit. The Veriti 96-Well Thermal Cycler real-time PCR system (Applied Biosystems, USA) quantified the relative mRNA levels. Table 1 displays the primers utilized in this study. We used the *GAPDH* gene as an internal standard. The $2^{-\triangle\triangle Ct}$ comparison technique was employed to analyze the data as per the procedures described previously

Table 1
The sequence of primers used for qRT-PCR in the present study.

Gene	Primer Sequence (5′→3′)	
TNF-α	F: ACGGCATGGATCTCAAAGAC	R: GTGGGTGAGGAGCACGTAGT
IL-1β	F: GCTGCTTCCAAACCTTTGAC	R: AGCTTCTCCACAGCCACAAT
IL-6	F: CCGGAGAGGAGACTTCACAG	R: CAGAATTGCCATTGCACAAC
p65	F: AGGCTTCTGGGCCTTATGTG	R: TGCTTCTCTCGCCAGGAATAC
IκB	F: ACAGCCAGGAGATGGTACG	R: CAGGGTGACTGAGTCGAGAC
GAPDH	F: AGGTCGGTGTGAACGGATTTG	R: TGTAGACCATGTAGTTGAGGTCA

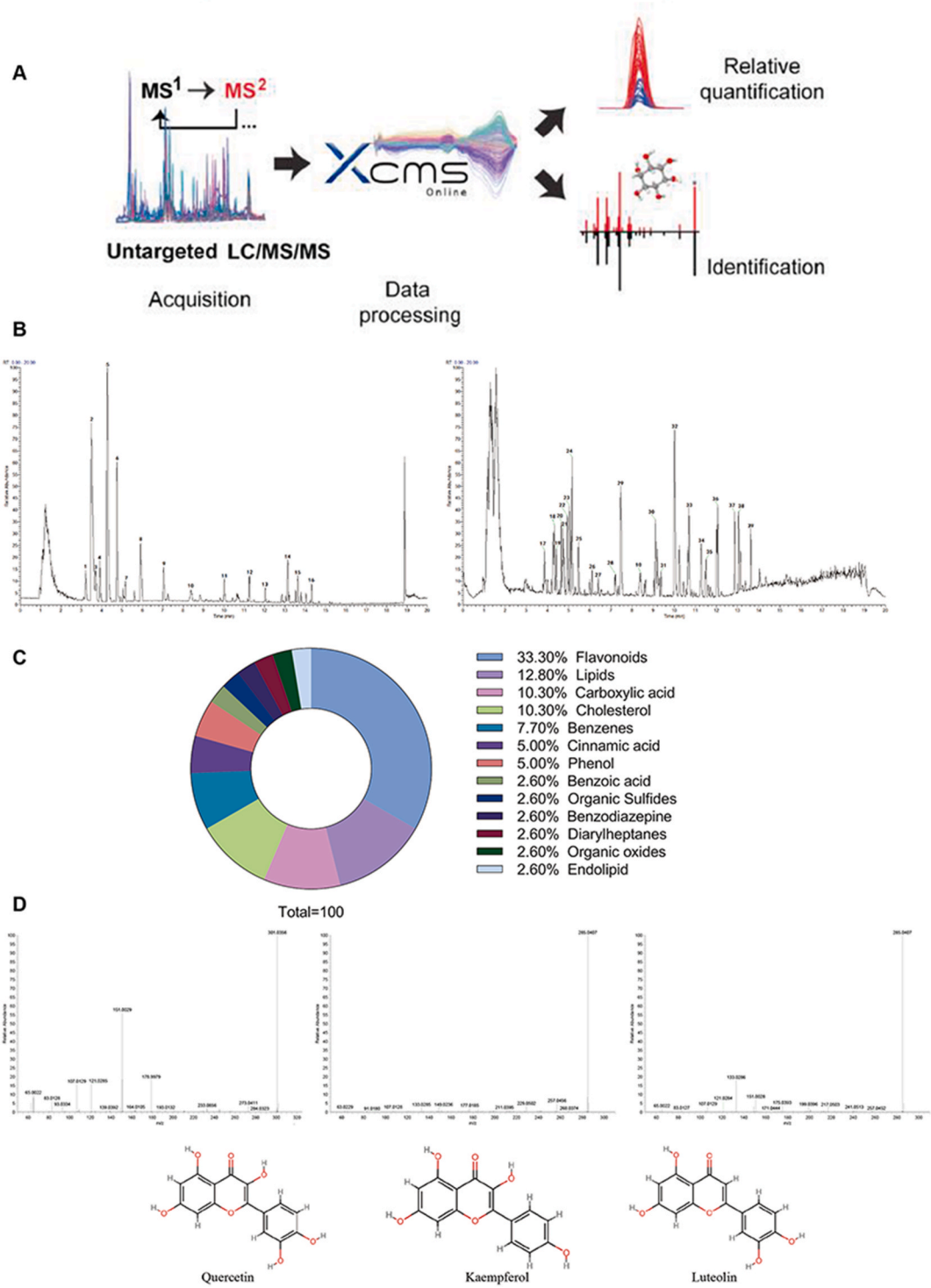

Fig. 2. JWYHD chemical composition identification. (A) Ingredient analysis process. (B) JWYHD's total ion chromatogram was observed in both the positive and negative ion phases. (C) Categorization statistics of 39 peak-paired compounds.(D) Secondary mass spectrum of some of the compositions and the main chemical components' molecular formula.

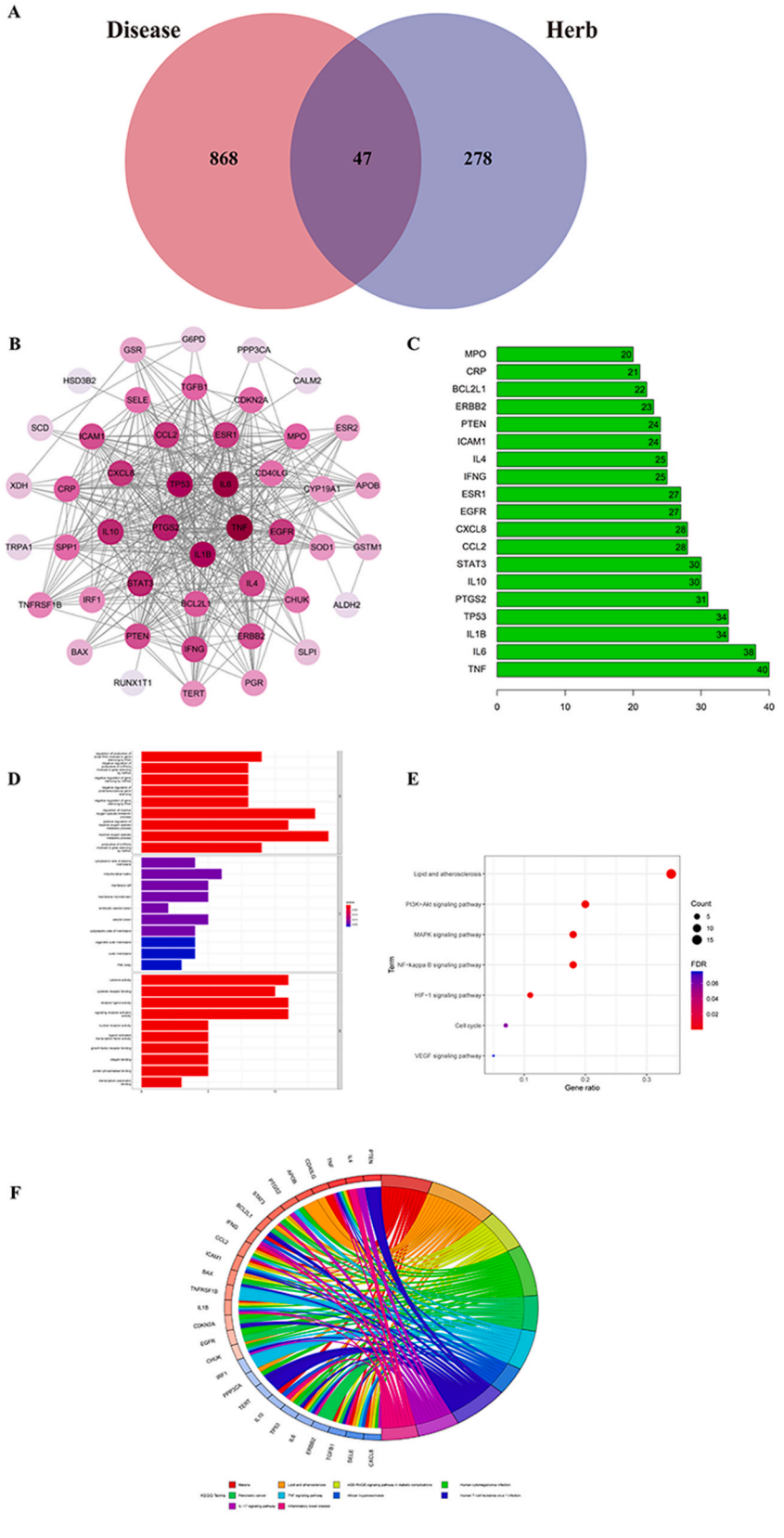

(caption on next page)

Fig. 3. (A)Venn diagram depicting the potential targets in LM.(B)PPI. The circle grows larger and the color shifts from light to black with increasing degrees of targets. The combined line enlarges with increasing combined total. (C) The degree number. The column length increased with increasing numbers. (D) Histogram of GO-enrichment analysis of the targets. (E) A bubble diagram of the targets' KEGG enrichment analysis. (F) Circos diagram of the 10 frequent targets' KEGG pathway enrichment analysis.

[37].

2.16. Western blotting

The RIPA buffer was used to remove the protein in accordance with the manufacturer's instructions. A polyvinylidene difluoride membrane was filled with sample proteins from the frozen mammary gland tissues (20 g), which was then treated with 5 % BSA in TBST for 4 h before rinsing thrice. Next, the membranes were treated with primary antibodies overnight at 4 °C.

Next, the membrane was treated with secondary antibodies for 1 h at room temperature after washing with TBST. The expression of the proteins was analyzed by using a chemiluminescence imaging device (Tanon, Shanghai, China).

2.17. Statistical analysis

GraphPad Prism 9.4.1 and ImageJ were used for the statistical analysis of the data. Tukey's multiple comparison tests and one-way analysis of variance (ANOVA) were employed to analyze the results for all groups. The results were presented as the mean ± standard error of the averages from 3 separate trials (SEM). $P < 0.05$ was considered to indicate statistical significance (*,*$P < 0.05$, **$P < 0.01$, and ***$P < 0.001$, relative to the LPS group; #$P < 0.05$, ##$P < 0.01$, and ###$P < 0.001$, relative to the blank control group).

3. Results

3.1. Determining JWYHD chemical composition

UPLC-HRMS and comparative abundance analyses were performed to determine the chemical composition of JWYHD. The Ingredient analysis process showed in Fig. 2A. The chromatographic and mass spectrometric conditions followed are described in Section 2.1. The chromatograms were scanned in both the positive and negative ion modes, as shown in Fig. 2B. Based on the information on quasi-molecular and characteristic fragment ions obtained by MS, combined with the standard spectrogram database matching, a total of 103 compounds were identified. The proportions of the top six classes of compounds and the number of their subclasses are shown in Supplementary Table 1. The peaks with higher abundance in the base peak chromatogram were checked for peak shape and confirmed by secondary spectra, and the 39 peaks in the positive and negative ion chromatograms, indicating phenylpropanoids, benzenes, carboxylic acids, cinnamic acids, flavonoids, and other components were labeled in numerical order (Fig. 2B). The compounds detected in the 39 chromatographic peaks were categorized and analyzed, of which flavonoids accounted for approximately 33.3 % (Figs. 2C), and 39 specific chemical constituents were identified, as listed in Supplementary Table 1. Among them, the structure-type representative components were selected separately, and the compounds were identified based on the primary and secondary MS data. The secondary mass spectra of some compounds are shown in Fig. 2D.

3.2. Network pharmacology-based screening of JWYHD components and LM-related targets

After the screening, we included 691 active components of JWYHD, including 25 RGD, 20 CEL, 13 ZOR, 171 CCD, 269 ESS, 46 SA, 23 GVS, 38 LJH, and 86 GUF. In the supplementary material, some of the active components are illustrated. Of these 691 active components, target prediction was performed, and 325 active components were extracted after deweighting.

Based on searches in GeneCards, OMIM, Disgenet, and DrugBank databases, 915 LM-related ensemble targets were identified and mapped onto the predicted targets of JWYHD active components, yielding 47 target–component interactions (Fig. 3A).

3.3. PPI network

For PPI network analysis, String (https://string-db.org) was used to load the 47 JWYHD–LM target–component interactions. In the PPI network, 47 nodes interacted via 400 edges, with an average local clustering coefficient of 0.717. The p-value for the PPI concentration was $<1.0e^{-16}$. Additionally, the "CentiScape" plug-in was used to calculate the "degree" value of each node; the greater the value, the greater the node's importance in the network. In the active component node group, the five main compounds were quercetin, kaempferol, luteolin, naringenin, and isorhamnetin, with the "degree" values of 35, 15, 14, 8, and 7, respectively, indicating them as essential components of the network. TNF-α, IL-6, IL-1β, tumor protein 53 (TP53), and prostaglandin G/H synthase 2 (PTGS2) were the five main targets in the target gene node group (Fig. 3B and C), and their corresponding "degree" values were 40, 38, 34, 34, and 31, respectively, indicating them as the network core.

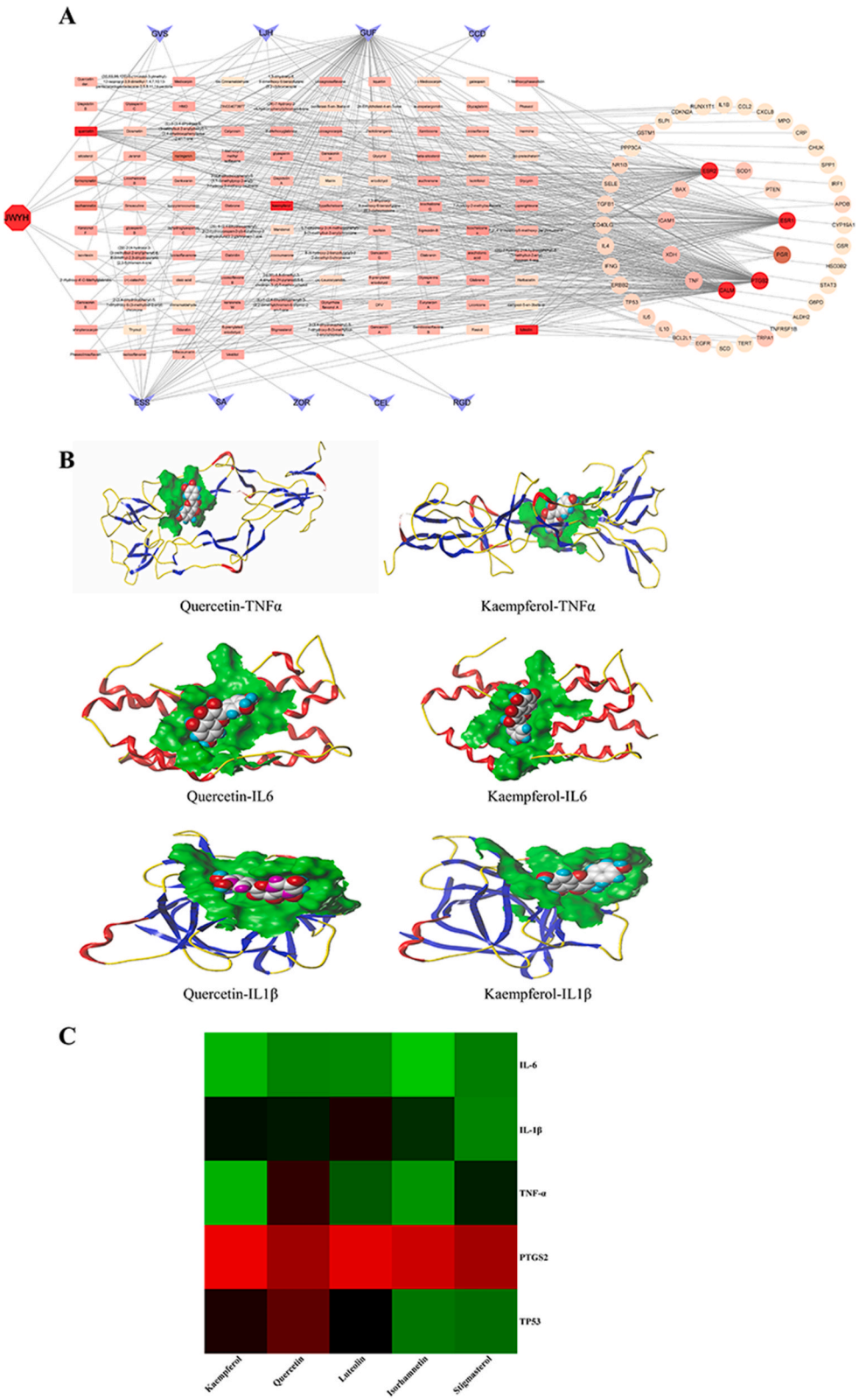

Fig. 4. (A)The compound–target-pathway network of JWYHD. The red circular nodes in this network represent the key targets, the blue nodes represent the JWYHD drug composition, the red quadrilateral represents the active ingredients of JWYHD, and the connecting lines represent the interaction among the three. (B) Models for the principal chemical substances' molecular interaction. (C) The absolute score of the docking affinity.

3.4. Gene function and pathway analysis

GO enrichment analysis included 1722 biological processes (BPs), 12 cellular components, 52 molecular functions, and 118 KEGG-related pathways, and the R language 3.6.2 program was used to extract information based on packets such as Bioconductor, with the threshold set to $P < 0.05$. The GO enrichment analysis results and KEGG-related pathways with high significance and relevance to this study were visualized.

Fig. 3D shows that JWYHD intervention in mastitis mainly involves the BP of the metabolism of reactive oxygen species and the regulation of inflammatory responses. Fig. 3E shows the results of the KEGG pathway analysis, which shows the top six signaling pathways of JWYHD for mastitis, and the key pathways are phosphoinositide-3-kinase/protein kinase B (PI3K-Akt) signaling pathway, mitogen-activated protein kinase signaling pathway, nuclear factor-kappa B (NF-κB) signaling pathway. The GO enrichment analysis results and KEGG-related pathways that are relevant and significant to this study were visualized (Fig. 3F).

3.5. Drug–active ingredient–target intersection

The 47 intersecting target genes of JWYHD for LM were mapped onto the screened active ingredients of JWYHD (some of the active ingredients did not match the corresponding targets) to establish a correspondence between the active ingredients and target genes. The results were imported into the Cytoscape 3.8.0 software to construct a "drug–target" regulatory network based on equality and properties. Finally, the results were imported into the Cytoscape 3.8.0 software to establish a "drug–active ingredient–target" regulatory network based on the correspondence and properties (Fig. 4A). The larger area of the nodes and the darker color in the diagram indicate their greater effect on mastitis.

3.6. Subdocking simulation

The results showed that three compounds, namely kaempferol, quercetin, and luteolin are the potential vital active ingredients in JWYHD. The top five target proteins in the core network that showed the highest "degree" values were TNF, IL-6, IL-1β, PTGS2, and TP53. Two-by-two match was made between the corresponding ingredients and targets. The stability and total score increased as the free binding energy of a receptor and ligand decreased. A total score ≥5.0 indicated that the critical activities of the ligand and target protein corresponded more closely. Therefore, both ligands and receptors were selected for molecular docking (Fig. 4B).

Quercetin showed binding energies of 6.3705, 4.1531, and 5.4704 for TNF-α, IL-6, and IL-1, respectively. In contrast, the critical

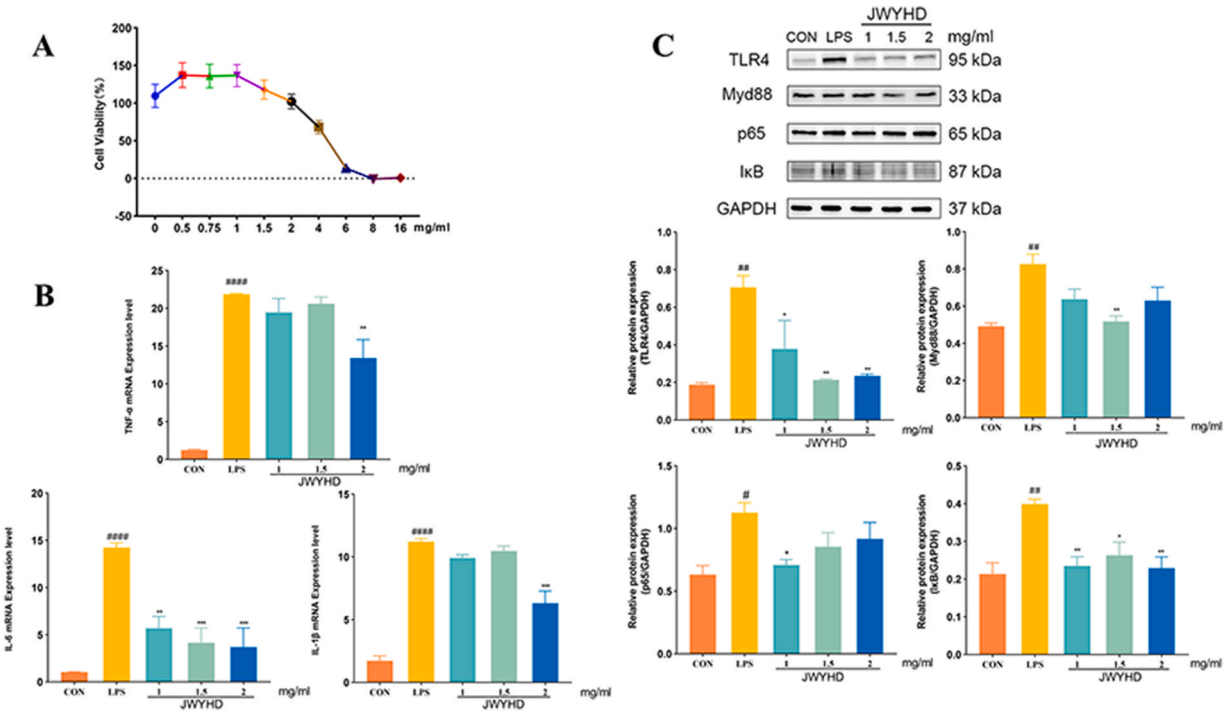

Fig. 5. (A) CCK-8 cell viability results of JWYHD. (B) mRNA expression of IL-1β, IL-6, and TNF-α for JWYHD.(C) Expression of key proteins of the TLR4/NF-κB signaling pathway for JWYHD. Data is expressed as the mean ± standard error, and three independent replicate experiments were performed, and with $P < 0.05$ were considered to indicate statistical significance. When compared with the LPS group, $^{*}P < 0.05$, $^{**}P < 0.01$, and $^{***}P < 0.001$. When compared with the control group, $\#P < 0.05$, $\#\#P < 0.01$, and $\#\#\#P < 0.001$.

ratios of kaempferol to TNF-α, IL-6, and IL-1β were 3.4587, 3.3955, and 5.5462, respectively (Fig. 4C).

3.7. Cell experiment

3.7.1. Effects of JWYHD on cell viability

CCK-8 assay was performed to evaluate the effect of JWYHD on HC11 activity. JWYHD at concentrations of 1, 1.5, or 2 mg/mL did not affect the cell viability (Fig. 5A).

3.7.2. Effect of JWYHD on LPS-induced pro-inflammatory factors in mammary epithelial cells

The levels of pro-inflammatory cytokines were elevated in HC11 treated with lipopolysaccharide when compared to the blank control cells. In the groups treated with JWYHD (1,1.5, and 2 mg/mL), the relative expression of pro-inflammatory factors (TNF-α, IL-6 and IL-1β) transcriptional mRNA revealed a downregulation trend when compared to that in the LPS group (Fig. 5B); these results indicated that JWYHD could regulate the lipopolysaccharide-induced elevation of inflammatory factor levels in the mammary epithelial cells.

3.7.3. JWYHD alleviates LPS -induced inflammatory response in mammary epithelial cells via NF-κB pathway

LPS stimulation increased the TLR4 expression in cells and inhibited TLR4, Myd88 expression by JWYHD pretreatment of cells (Fig. 5C). The NF-κB pathway can be involved in the inflammatory process. In HC11 cells, LPS stimulation induced a significant increase in the IκB expression and the p65 protein expressions, and JWYHD inhibited these increases. These results suggest that JWYHD responded to LPS-induced elevation of the IκB and p65 protein levels in the mammary epithelial cells.

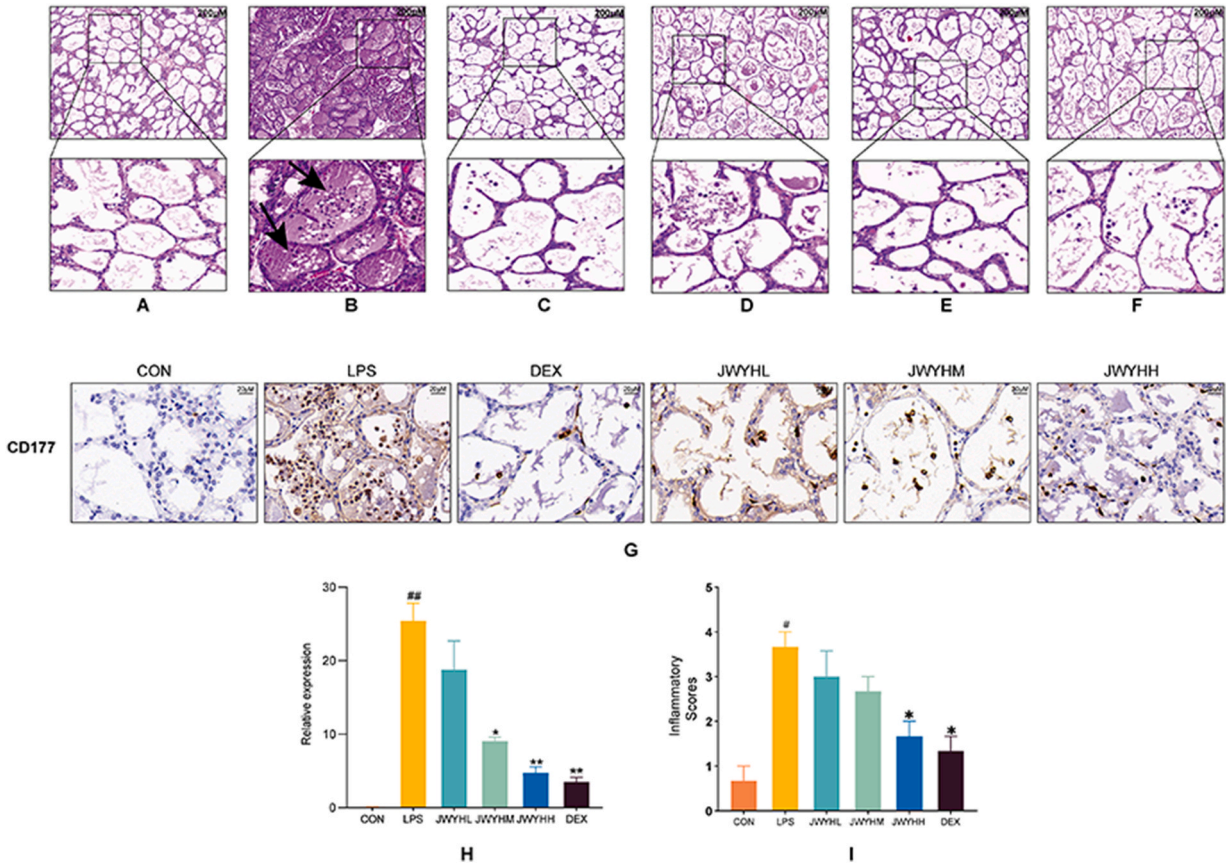

Fig. 6. Pathological, histological, and immunohistochemical effects of JWYHD. (A–F) Mammary tissue slices stained with H&E; Scale bar: 200 M; Magnification: 50×. (I) The scores of pathological injury. (G–H) The CD177 expression was examined by immunohistochemistry in the mammary tissues of different LM mice. Three independent replicate experiments were conducted, and the results were expressed as the mean ± standard error, with $P < 0.05$ considered to indicate statistical significance. When compared to the LPS group, $^{*}P < 0.05$, $^{**}P < 0.01$, and $^{***}P < 0.001$. When compared to the blank control group, $\#P < 0.05$, $\#\#P < 0.01$, and $\#\#\#P < 0.001$.

3.8. Animal experiments

3.8.1. Pathological histological and immunohistochemical effects of JWYHD on mammary glands of mice

To further verify the anti-inflammatory effect of JWYHD and to explore the possible underlying mechanism, we established a mastitis model in lactating BALB/c mice. Histopathological changes in the mammary glands of mice in each group were first observed by hematoxylin–eosin (HE) staining (Fig. 6A–F), followed by immunohistochemical staining to assess the level of the inflammatory cytokine CD177 in mammary gland tissues (Fig. 6G and H). The findings suggested that no obvious pathological changes were observed in the blank control group; however, the mammary tissue structure of mice in the LPS group showed considerable damage, including atrophy or even necrosis of glandular follicles and a significant infiltration of neutrophilic leukocytes into the glandular lumen. The damage to mammary tissues was significantly reduced by pretreatment with JWYHD (Fig. 6I), which effectively and significantly reduced mastitis in mice exposed to LPS. The effect of JWYHD on mastitis was comparable to that of DEX, which effectively and significantly reduced histological changes in inflammation in mice with LPS-induced mastitis.

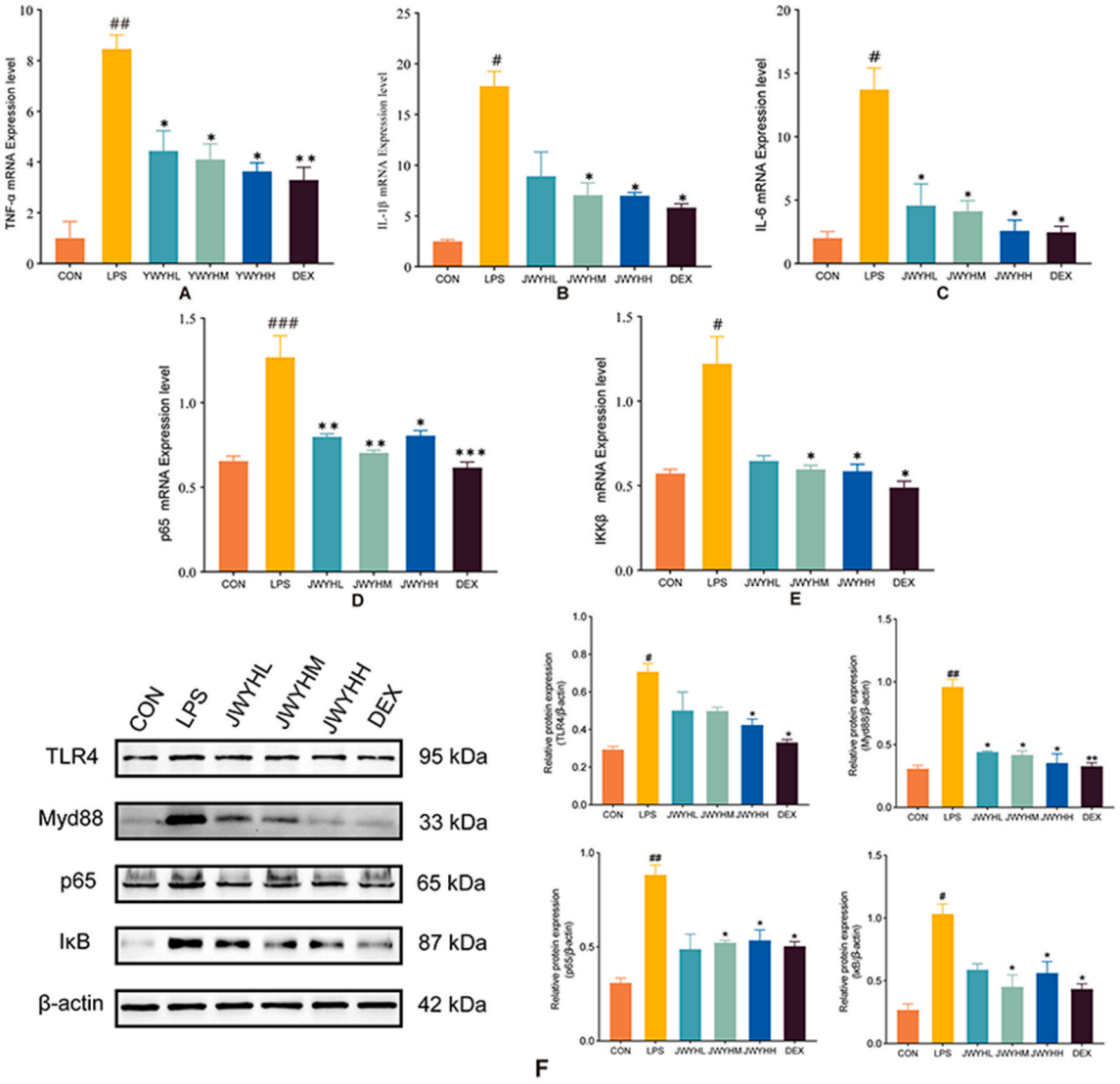

Fig. 7. JWYHD's mammary gland inflammatory responses on the TLR4/Myd88/NF-κB pathway. (A–E) JWYHD intervention reduced the expression of TNF-α, IL-6, IL-1β, p65, and IκB in the breast tissues, as measured by real-time fluorescence quantitative PCR technique. (F) Western blotting of the expression of TLR4, Myd88, NF-κB, p65, and IκB in the breast tissues. Expressed as the mean ± standard error, three independent replicate experiments were performed, and $P < 0.05$ were considered to indicate statistical significance. When compared with the LPS group, $*P < 0.05$, $**P < 0.01$, and $***P < 0.001$. When compared with the blank control group, $\#P < 0.05$, $\#\#P < 0.01$, and $\#\#\#P < 0.001$.

3.8.2. JWYHD inhibited mammary gland inflammatory responses and downregulated the TLR4/Myd88/NF-κB pathway in mice

Similar to the pre-informatics results, JWYHD affected the expression of mastitis-related genes and proteins by regulating the TLR4/Myd88/NF-κB pathway. The PCR results showed significantly increased TNF-α, IL-6, IL-1β, p65, and IκB levels in the mammary tissues of the LPS-induced mice ($P < 0.05$). JWYHD intervention decreased this increase ($P < 0.05$) (Fig. 7A–E). p65 and IκB were the key targets of the TLR4/Myd88/NF-κB signalling pathway, and TNF-α, IL-6, and IL-1β were also involved in it as the main downstream inflammatory factors.

Western blotting showed that LPS stimulation increased TLR4, Myd88, p65, and IκB levels, whereas these increased levels decreased significantly after JWYHD treatment (Fig. 7F). We determined a possible association between the JWYHD treatment of mastitis and this signaling pathway by analyzing the effect of different drug concentrations on the TLR4/Myd88/NF-κB signaling pathway in LPS-stimulated inflamed tissues. The results validated our assumptions. Thus, JWYHD may act on mastitis tissues via the TLR4/Myd88/NF-κB signalling pathway.

3.8.3. JWYHD significantly reduced mammary gland inflammatory factors and myeloperoxidase (MPO) levels

ELISA was performed to quantify the levels of IL-1β, IL-6, TNF-α, and MPO in breast tissues. Compared with the blank control group, the levels of all three inflammatory cytokines increased significantly in the LPS group mice (Fig. 8A–C); however, the levels of the three inflammatory factors decreased significantly after JWYHD treatment (Fig. 8A–C). The results indicated that JWYHD could attenuate the LPS-induced inflammatory response in the mammary glands of these mice. Similarly, MPO activity was significantly higher in the LPS group than in the blank control group (Fig. 8D, $P < 0.01$). As expected, the JWYHD pretreatment group showed significantly reduced MPO activity.

4. Discussion

In the last decade, China has ranked among the world's top producers and consumers of antibiotics [38,39]. The resulting bacterial resistance and the continued expansion of consumption create a vicious cycle. Thus, reducing antibiotics, bridging the gap between developing and developed nations, and improving medical care to benefit humans and nature must be considered. In this context,

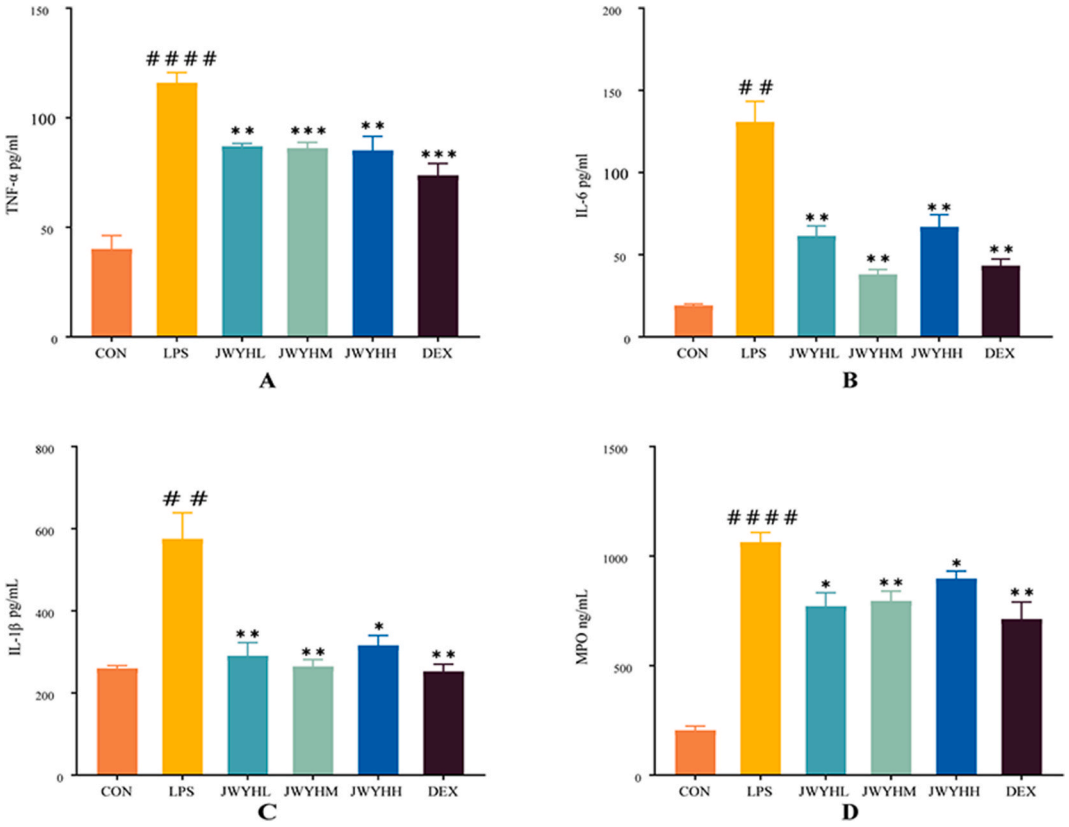

Fig. 8. Effect of JWYHD on the expression of pro-inflammatory cytokines in the mammary tissues. (A–D) Effect of JWYHD on the expression of pro-inflammatory cytokines in the mammary tissues. The expression of IL-1β, IL-6, and TNF-α, MPO in the breast tissues was measured by ELISA. Data expressed as the mean ± standard error and three independent replicate experiments were performed, with $P < 0.05$ were considered to indicate statistical significance. When compared with the LPS group, $^{*}P < 0.05$, $^{**}P < 0.01$, and $^{***}P < 0.001$. When compared with the blank control group, $\#P < 0.05$, $\#\#P < 0.01$, and $\#\#\#P < 0.001$.

Chinese medicine has played a unique role in treating inflammatory diseases. By reversing bacterial resistance, the synergistic effect of TCM and antibiotics can enhance anti-inflammatory and antibacterial effects, thereby reducing the need for antibiotics [40–42]. The TCM mode of action in mastitis treatment may involve directly killing the pathogen directly, regulating systemic functions, and reshaping the imbalance, thus exerting an irreversible anti-inflammatory effect.

The original YHD formula has a long history of application. Moreover, its modified formulas can be used for extensive clinical therapies for refractory and recurrent refractory diseases, such as chronic inflammatory diseases, autoimmune diseases, and even tumour-related diseases [26–28]. In the clinical treatment of acute mastitis, this study found that the overall effective rate of YHD combined treatments was higher than in the control group [43]. According to Chinese medicine theory, the warmth of *Yang qi* facilitates the performance of human external life activities in a normal and orderly manner. Since breasts belong to the foot or "Yang-ming" stomach meridian and nipples belong to the foot syncope yin liver meridian, treatment of acute mastitis should focus on the *blood* and *qi*, as per the physiological state of Sufficient *Yang*. Thus, breast disease treatment should principally include warming *Yang*. Considering the physiological characteristics of LM patients at a specific time, the addition of two herbs seems more suitable for successful clinical application. *Yang* is warmed to replenish blood and essence as well as cultivate the spleen and earth so that the resultant meridians become smooth, whilst *qi*, blood flow, cold dissipate and phlegm disappears. The warming effect of JWYHD is significant compared with traditional heat-clearing formulas e.g., Gualou Niubang soup and Chaihu Qinggan soup. Therefore, this study was discussed in terms of content and results in the following aspects.

4.1. UPLC-HRMS and network pharmacology

Network pharmacology was combined with UPLC-HRMS. A variety of chemical components were screened and compared with UPLC-HRMS results to obtain several functioning compounds, e.g., quercetin, kaempferol, and luteolin. From an analysis of their compound categorisations, flavonoids were found to occupy the main position among the components of JWYHD (Fig. 2C). As parts of flavonoids, quercetin and kaempferol can resist reactive oxygen scavenging, enhance plant defence responses, and show anti-inflammatory and antioxidant effects [44]. The anti-inflammatory and immunomodulatory properties of quercetin and kaempferol, the herb components with diverse biological properties, have been widely studied in multiple inflammatory events [45], which suggests that JWYHD may be essential for suppressing inflammatory diseases characterised by the immune system. Quercetin and kaempferol exhibit potent anti-inflammatory and antimicrobial properties [46,47]. Several studies have demonstrated that quercetin can protect cells from IL-1β stimulation via inhibition of NF-κB activation [48]. In a skin inflammation model, quercetin suppressed the inflammatory eruption induced by LPS-activated macrophages, thereby decreas TNF-α, IL-1β, and IL-6 levels [49]. Moreover, kaempferol can regulate proinflammatory cytokine levels by inhibiting neutrophil accumulation and MPO activity [50]. in addition, it can reduce LPS-induced TNF-α and IL-1β levels by increasing the number of activated macrophages, whereas TNF-α inhibition mediates the nuclear translocation of NF-κB p65 [51]. Moreover, we simulated the molecular docking of five protein-coding genes with two noteworthy compounds, and the results revealed that all target compounds were docked with a high affinity. Considering the complexity of the herbal compound and the synergistic effect of multiple ingredients, quercetin, and kaempferol were used to enhance the potency of JWYHD as enriched ingredients in this formula.

4.2. Mechanism of action

To further investigate the mechanism underlying the role of JWYHD, network pharmacology screening was performed. Results suggested that TNF-α, IL-6, and IL-1β were highly correlated with mastitis and were possible potential key targets. The gene and pathway enrichment analyses showed that the PI3K-AKT and NF-κB signalling pathways were strongly associated with inflammation. The relationship between inflammation and cancer has been widely studied, and the level of inflammatory factors in a tumour microenvironment has been associated with the levels of proteins involved in the PI3K-AKT signalling pathway, which exacerbates the development of cancer and is closely associated with cancerous tumours [52]. However, this was not the focus of the present study. The LPS/NF-κB signalling pathway has been closely associated with biological inflammation [53].,where LPS acts as a bacterial virulence factor. In the current model, LPS-specific activated cells could bind to receptors on the surface of mammary epithelial cells [54], thereby triggering NF-κB nuclear translocation to regulate inflammation-related genes [55,56]. Moreover, TLRs can trigger the NF-κB signalling pathway to regulate the transcription of inflammatory mediators specific to mammary epithelial cell inflammation [57,58]. When mastitis-induced bacteria activate TLRs, they can signal Myd88 and cause a cascade of responses. Myd88 is a key regulator of NF-κB can lead to IκB degradation, and is considered to be a key immunomodulatory adapter molecule against various pathogens [59, 60]. The classical NF-κB pathway can be activated within a few minutes of exposure to pro-inflammatory signals (e.g., cytokines), with p65:p50 heterodimers being the most abundant manifestation of this signalling pathway upon activation [61]. It mediates inflammation by activating the IKKB complex, leading to the degradation of classical IκB (IκBα, IκBβ, or IκBε) and the subsequent release of NF-κB dimers for nuclear translocation [62–64]. Thus, activated p65 and IκB are key elements in inflammatory disease pathogenesis.

4.3. In vivo and in vitro effects

The aqueous decoction of JWYHD exerted an excellent anti-inflammatory effect in vivo and in vitro and could effectively reduce TNF-α, IL-1β, and IL-6 levels (Fig. 7A–C). Cytokines are indispensable for intercellular communication and they regulate immune cell activity and inflammatory signalling responses [52]. TNF-α, IL-1β, and IL-6 are pleiotropic proinflammatory cytokines that are deemed crucial for disease pathogenesis and dynamic homeostasis, and they are involved in several BPs, including necrosis, apoptosis, and

inflammation [65,66]. MPO is a peroxidase present in and secreted by activated leukocytes that may be directly or indirectly involved in tissue damage [67]. CD177 acts as an adhesion molecule in the presence of endothelial cells and is involved in a neutrophil endothelial cell adhesion and neutrophil migration [68], which are upregulated on the surface of neutrophils after severe bacterial infections and granulocyte colony-stimulating factor stimulation [69]. Results suggested that JWYHD could reduce neutrophil aggregation in the mammary gland by reducing MPO activity and immunohistochemical CD177 in LPS-induced mastitis(Figs. 6G and 8D). This result indicates that JWYHD can prevent mastitis by reducing the level of these proinflammatory cytokines and inflammatory markers.

HE staining and immunohistochemistry objectively revealed that JWYHD could play a certain therapeutic role in reducing the degree of inflammatory infiltration and the damage score level of breast tissues at the microscopic level. In this regard, the levels of IL-1β, IL-6, and TNF-α decreased significantly after JWYHD intervention. This indicates that JWYHD can reduce breast tissue inflammation by reducing the level of these proinflammatory cytokines. At the gene and protein levels, JWYHD exerted a significant effect by reducing the activation of key proteins in the TLR4/Myd88/NF-κB signalling pathway and downstream proteins. The therapeutic effects of JWYHD on mammary gland inflammation were investigated, and the results were consistent with the network pharmacological screening results. To summarize, this study showed the therapeutic efficacy of JWYHD in treating mastitis from multiple perspectives and at different levels, thus new evidence for promoting the clinical use of JWYHD in treating LM.

4.4. Limitations

Moreover, in clinical practice, we have observed that LM was observed to be often accompanied by lump accumulation after the acute phase, particularly after treatment with antibiotics, which may be a state of tolerance between the “inflammation” of the body and the “immunity” to eliminate it. These lumps disappeared more quickly after JWYHD application, leading to disease healing. Presently, anti-inflammatory drugs are often used as the first choice for achieving antibacterial effects. However, the overall medicinal property of JWYHD is on the warm side, treating the disease with warmth and warming and resolving blood stasis, which differents from other prescription groups. Although analyzing the target of action of JWYHD by network pharmacology was initially envisioned to determine if it was different from previous formulations. However, no distinction has been observed between the natures of the drug action molecules. After using JWYHD by UPLC-HRMS for preliminary identification of the in vitro chemical constituents and matching them with network pharmacology, further analysis and the study of the constituents after entering the blood were lacking. To induce a model of inflammation in mammary epithelial cells through LPS in cellular experiments, JWYHD observation at different time points was lacking. To observe the effect of JWYHD on its mechanism in animal experiments, the silencing of key proteins in the signalling pathway NF-κB and inflammatory vesicles was not applied. Due to limitations imposed by incomplete and unquantifiable data, network pharmacology could not be used to validate all the experiments on the multi-pathway targets involved in the study. Future studies are expected address these limitations in detail.

Generally, it is anticipated that the multi-herb, multi-compound, multi-target, and multi-channel characteristics of Chinese herbal formulas, combined with the comprehensive and systematic nature of modern network pharmacology, will serve as indispensable tools for investigating the unique effects of Chinese medicine. In this study, herbal medicine research was integrated with modern information technology. The results of network pharmacology prediction, molecular docking simulation, and in vivo and in vitro experiments were in alignment with the expected outcomes.

5. Conclusions

According to network pharmacology and molecular docking studies, the mechanism of the action of JWYHD in mastitis treatment involves regulating multiple biological pathways and targets. JWYHD reduces the levels of proinflammatory cytokines, such as TNF-α, IL-1β, and IL-6, by inhibiting the expression of the genes of p65 and IκB, the major proteins of the TLR4/Myd88/NF-κB signalling pathway. This ameliorates LPS-induced pathological changes mainly by neutrophil aggregation. Therefore, JWYHD can be used in clinical practice to obtain more robust evidence of its effectiveness in treating inflammatory diseases such as LM.

Declaration of competing interest

The authors declare that they have no known competing financial interests or personal relationships that could have appeared to influence the work reported in this paper.

Acknowledgements

This work was financially supported by grants from the Xiamen High Level Health Talents Introduction and Training Project (Xiaweidang 2021-124) and the Capital Health Development Research Special Project (2018-7032).

Appendix A. Supplementary data

Supplementary data to this article can be found online at https://doi.org/10.1016/j.heliyon.2023.e21219.

References

[1] L. Saiman, M. O'Keefe, P.L. Graham, F. Wu, P. Della-Latta, Hospital transmission of community-acquired methicillin-resistant Staphylococcus aureus among postpartum women, Clin. Infect. Dis. 37 (2003) 1313–1319.

[2] L.H. Amir, C. Academy of Breastfeeding Medicine Protocol, ABM clinical protocol #4: mastitis, revised March 2014, Breastfeed. Med. 9 (2014) 239–243. http://10.1089/bfm.2014.9984.

[3] R. Eryilmaz, M. Sahin, M. Hakan Tekelioglu, E. Daldal, Management of lactational breast abscesses, Breast 14 (2005) 375–379. http://10.1016/j.breast.2004.12.001.

[4] L.H. Amir, D. Forster, H. McLachlan, J. Lumley, Incidence of breast abscess in lactating women: report from an Australian cohort, BJOG 111 (2004) 1378–1381. http://10.1111/j.1471-0528.2004.00272.x.

[5] WHODo Child, A. Health, Development, Mastitis: Causes and Management, 2000.

[6] J.A. Scott, M. Robertson, J. Fitzpatrick, C. Knight, S. Mulholland, Occurrence of lactational mastitis and medical management: a prospective cohort study in Glasgow, Int. Breastfeed. J. 3 (2008) 21. http://10.1186/1746-4358-3-21.

[7] J.P. Spencer, Management of mastitis in breastfeeding women, Am. Fam. Physician 78 (2008) 727–731.

[8] L.E. Grzeskowiak, M.R. Saha, W.V. Ingman, H. Nordeng, E. Ystrom, L.H. Amir, Incidence, antibiotic treatment and outcomes of lactational mastitis: findings from the Norwegian mother, father and child cohort study (MoBa), Paediatr. Perinat. Epidemiol. 36 (2022) 254–263. http://10.1111/ppe.12824.

[9] Y. Zhao, X. Xiao, S.J. Frank, H.Y. Lin, Y. Xia, Distinct mechanisms of induction of hepatic growth hormone resistance by endogenous IL-6, TNF-alpha, and IL-1beta, Am. J. Physiol. Endocrinol. Metab. 307 (2014) E186–E198. http://10.1152/ajpendo.00652.2013.

[10] E.M. Paolucci, D. Loukov, D.M.E. Bowdish, J.J. Heisz, Exercise reduces depression and inflammation but intensity matters, Biol. Psychol. 133 (2018) 79–84. http://10.1016/j.biopsycho.2018.01.015.

[11] A. Ahmad, A.F. Wali, M.U. Rehman, A. Khan, M. Raish, M. Kazi, et al., Therapeutic Potential of Rhododendron Arboreum Polysaccharides in an Animal Model of Lipopolysaccharide-Inflicted Oxidative Stress and Systemic Inflammation. Molecules, 2020, p. 25. http://10.3390/molecules25246045.

[12] D. Diaz, E. Lopez-Dolado, S. Haro, J. Monserrat, C. Martinez-Alonso, D. Balomeros, et al., Systemic inflammation and the breakdown of intestinal homeostasis are key events in chronic spinal cord injury patients, Int. J. Mol. Sci. (2021) 22. http://10.3390/ijms22020744.

[13] H.F. Chambers, F.R. Deleo, Waves of resistance: Staphylococcus aureus in the antibiotic era, Nat. Rev. Microbiol. 7 (2009) 629–641. http://10.1038/nrmicro2200.

[14] M.V. Pirotta, J.M. Gunn, P. Chondros, "Not thrush again!" Women's experience of post-antibiotic vulvovaginitis, Med. J. Aust. 179 (2003) 43–46. http://10.5694/j.1326-5377.2003.tb05418.x.

[15] M.J. Dinsmoor, R. Viloria, L. Lief, S. Elder, Use of intrapartum antibiotics and the incidence of postnatal maternal and neonatal yeast infections, Obstet. Gynecol. 106 (2005) 19–22. http://10.1097/01.AOG.0000164049.12159.bd.

[16] S. Panda, I. El khader, F. Casellas, J. Lopez Vivancos, M. Garcia Cors, A. Santiago, et al., Short-term effect of antibiotics on human gut microbiota, PLoS One 9 (2014), e95476. http://10.1371/journal.pone.0095476.

[17] A. Langdon, N. Crook, G. Dantas, The effects of antibiotics on the microbiome throughout development and alternative approaches for therapeutic modulation, Genome Med. 8 (2016). http://10.1186/s13073-016-0294-z.

[18] J.A. Eisen, L. Dethlefsen, S. Huse, M.L. Sogin, D.A. Relman, The pervasive effects of an antibiotic on the human gut microbiota, as revealed by deep 16S rRNA sequencing, PLoS Biol. (2008) 6. http://10.1371/journal.pbio.0060280.

[19] L. Dethlefsen, D.A. Relman, Incomplete recovery and individualized responses of the human distal gut microbiota to repeated antibiotic perturbation, Proc. Natl. Acad. Sci. USA 108 (2010) 4554–4561. http://10.1073/pnas.1000087107.

[20] Samreen, F.A. Qais, I. Ahmad, Anti-quorum sensing and biofilm inhibitory effect of some medicinal plants against gram-negative bacterial pathogens: in vitro and in silico investigations, Heliyon 8 (2022), e11113. http://10.1016/j.heliyon.2022.e11113.

[21] Y.X. Zhou, X.Y. Cao, C. Peng, Antimicrobial activity of natural products against MDR bacteria: a scientometric visualization analysis, Front. Pharmacol. 13 (2022), 1000974. http://10.3389/fphar.2022.1000974.

[22] G. De, A. Chen, Q. Zhao, R. Xie, C. Wang, M. Li, et al., A multi-herb-combined remedy to overcome hyper-inflammatory response by reprogramming transcription factor profile and shaping monocyte subsets, Pharmacol. Res. 169 (2021), 105617. http://10.1016/j.phrs.2021.105617.

[23] C.Q. Zhao, Y. Zhou, J. Ping, L.M. Xu, Traditional Chinese medicine for treatment of liver diseases: progress, challenges and opportunities, J Integr Med 12 (2014) 401–408. http://10.1016/S2095-4964(14)60039-X.

[24] X. Cheng, K.H. Merz, The role of indirubins in inflammation and associated tumorigenesis, Adv. Exp. Med. Biol. 929 (2016) 269–290. http://10.1007/978-3-319-41342-6_12.

[25] C. Jing, L. Xinxin, L. Yang, W. Boyu, Y. Min, H. Zhitao, Research progress on indications of Yanghe decoction, Chinese Archives of Traditional Chinese Medicine 40 (2022) 10–13. http://10.13193/j.issn.1673-7717.2022.08.003.

[26] H. Xia, D. Cao, F. Yang, W. Yang, W. Li, P. Liu, et al., Jiawei Yanghe decoction ameliorates cartilage degradation in vitro and vivo via Wnt/beta-catenin signaling pathway, Biomed. Pharmacother. 122 (2020), 109708. http://10.1016/j.biopha.2019.109708.

[27] C. Li, L. Tian, Y. Jiang, Y. Wang, L. Xue, S. Zhang, et al., Yanghe decoction effectively alleviates lung injury and immune disorder in asthmatic mice induced by ovalbumin, Comput. Intell. Neurosci. 2022 (2022), 6040575. http://10.1155/2022/6040575.

[28] B. Ma, D. Chen, Y. Liu, Z. Zhao, J. Wang, G. Zhou, et al., Yanghe decoction suppresses the experimental autoimmune thyroiditis in rats by improving NLRP3 inflammasome and immune dysregulation, Front. Pharmacol. 12 (2021), 645354. http://10.3389/fphar.2021.645354.

[29] L. Yan, L. Li-hua, W. Xing-de, The effect of Yanghe decoction on TNF- α of patients with acute mastitis, Health Research 35 (2015) 511–512+5.

[30] J. Ru, P. Li, J. Wang, W. Zhou, B. Li, C. Huang, et al., TCMSP: a database of systems pharmacology for drug discovery from herbal medicines, J. Cheminf. 6 (2014) 13. http://10.1186/1758-2946-6-13.

[31] J. Pinero, J.M. Ramirez-Anguita, J. Sauch-Pitarch, F. Ronzano, E. Centeno, F. Sanz, et al., The DisGeNET knowledge platform for disease genomics: 2019 update, Nucleic Acids Res. 48 (2020) D845–D855. http://10.1093/nar/gkz1021.

[32] T. Chen, H. Zhang, Y. Liu, Y.X. Liu, L. Huang, EVenn: easy to create repeatable and editable Venn diagrams and Venn networks online, J Genet Genomics 48 (2021) 863–866. http://10.1016/j.jgg.2021.07.007.

[33] L.J. Crofford, B. Tan, C.J. McCarthy, T. Hla, Involvement of nuclear factorkB in the regulation of cyclooxygenase-2 expression by interleukin-1 in rheumatoid synoviocytes, Arthritis Rheum. 40 (1997) 226–236. http://10.1002/art.1780400207.

[34] E.A. Mazzio, N. Li, D. Bauer, P. Mendonca, E. Taka, M. Darb, et al., Natural product HTP screening for antibacterial (E.coli 0157:H7) and anti-inflammatory agents in (LPS from E. coli O111:B4) activated macrophages and microglial cells; focus on sepsis, BMC Compl. Alternative Med. 16 (2016). http://10.1186/s12906-016-1429-x.

[35] J-l Lai, Y-h Liu, Y-c Peng, P. Ge, C-f He, C. Liu, et al., Indirubin Treatment of Lipopolysaccharide-Induced Mastitis in a Mouse Model and Activity in Mouse Mammary Epithelial Cells, Mediators of Inflammation, 2017, pp. 1–13, 2017, http://10.1155/2017/3082805.

[36] W. Guo, B. Liu, G. Hu, X. Kan, Y. Li, Q. Gong, et al., Vanillin protects the blood-milk barrier and inhibits the inflammatory response in LPS-induced mastitis in mice, Toxicol. Appl. Pharmacol. 365 (2019) 9–18. http://10.1016/j.taap.2018.12.022.

[37] J.L. Lai, Y.H. Liu, C. Liu, M.P. Qi, R.N. Liu, X.F. Zhu, et al., Indirubin inhibits LPS-induced inflammation via TLR4 abrogation mediated by the NF-kB and MAPK signaling pathways, Inflammation 40 (2017) 1–12. http://10.1007/s10753-016-0447-7.

[38] E.Y. Klein, M. Milkowska-Shibata, K.K. Tseng, M. Sharland, S. Gandra, C. Pulcini, et al., Assessment of WHO antibiotic consumption and access targets in 76 countries, 2000-15: an analysis of pharmaceutical sales data, Lancet Infect. Dis. 21 (2021) 107–115. http://10.1016/S1473-3099(20)30332-7.

[39] X. Liu, S. Lu, W. Guo, B. Xi, W. Wang, Antibiotics in the aquatic environments: a review of lakes, China, Sci. Total Environ. 627 (2018) 1195–1208. http://10.1016/j.scitotenv.2018.01.271.

[40] Q.Q. Liu, J. Han, G.Y. Zuo, G.C. Wang, H.S. Tang, Potentiation activity of multiple antibacterial agents by Salvianolate from the Chinese medicine Danshen against methicillin-resistant Staphylococcus aureus (MRSA), J. Pharmacol. Sci. 131 (2016) 13–17. http://10.1016/j.jphs.2015.10.009.
[41] C.R. Bi, W. Jing, X.F. Xie, Y.J. Liu, Efficacy and mechanism of traditional Chinese medicine in relieving antibiotic-resistant bacterial diarrhea in children: study protocol for a randomized controlled trial, Trials 22 (2021) 426. http://10.1186/s13063-021-05381-8.
[42] S. Qu, C. Dai, Z. Shen, Q. Tang, H. Wang, B. Zhai, et al., Mechanism of synergy between tetracycline and quercetin against antibiotic resistant Escherichia coli, Front. Microbiol. 10 (2019) 2536. http://10.3389/fmicb.2019.02536.
[43] X.G. Yun Chen, Clinical observation on the treatment of acute mastitis in the stagnant stage by combining the warm-passing method with manipulation to pass the breastmilk, Zhejiang JITCWM 29 (2019) 159–161.
[44] Z. Lei, B.W. Sumner, A. Bhatia, S.J. Sarma, L.W. Sumner, UHPLC-MS Analyses of Plant Flavonoids. Current Protocols in Plant Biology, vol. 4, 2018. http://10.1002/cppb.20085.
[45] C.L. Tian, X. Liu, Y. Chang, R.X. Wang, T.M. Lv, C.C. Cui, et al., Investigation of the anti-inflammatory and antioxidant activities of luteolin, kaempferol, apigenin and quercetin, South Afr. J. Bot. 137 (2021) 257–264. http://10.1016/j.sajb.2020.10.022.
[46] M. Chagas, M.D. Behrens, C.J. Moragas-Tellis, G.X.M. Penedo, A.R. Silva, C.F. Goncalves-de-Albuquerque, Flavonols and flavones as potential anti-inflammatory, antioxidant, and antibacterial compounds, Oxid. Med. Cell. Longev. 2022 (2022), 9966750. http://10.1155/2022/9966750.
[47] S.A. Jones, B.J. Jenkins, Recent insights into targeting the IL-6 cytokine family in inflammatory diseases and cancer, Nat. Rev. Immunol. 18 (2018) 773–789. http://10.1038/s41577-018-0066-7.
[48] S.C. Cheng, W.C. Huang, S.P. Jh, Y.H. Wu, C.Y. Cheng, Quercetin inhibits the production of IL-1beta-induced inflammatory cytokines and chemokines in ARPE-19 cells via the MAPK and NF-kappaB signaling pathways, Int. J. Mol. Sci. (2019) 20. http://10.3390/ijms20122957.
[49] J. Tang, P. Diao, X. Shu, L. Li, L. Xiong, Quercetin and quercitrin attenuates the inflammatory response and oxidative stress in LPS-induced RAW264.7 cells: in vitro assessment and a theoretical model, BioMed Res. Int. 2019 (2019), 7039802. http://10.1155/2019/7039802.
[50] Q. Li, X. Hu, Y. Xuan, J. Ying, Y. Fei, J. Rong, et al., Kaempferol protects ethanol-induced gastric ulcers in mice via pro-inflammatory cytokines and NO, Acta Biochim. Biophys. Sin. 50 (2018) 246–253. http://10.1093/abbs/gmy002.
[51] M.K. Lin, Y.L. Yu, K.C. Chen, W.T. Chang, M.S. Lee, M.J. Yang, et al., Kaempferol from Semen cuscutae attenuates the immune function of dendritic cells, Immunobiology 216 (2011) 1103–1109. http://10.1016/j.imbio.2011.05.002.
[52] Z.P. Espinosa-Riquer, D. Segura-Villalobos, I.G. Ramirez-Moreno, M.J. Perez Rodriguez, M. Lamas, C. Gonzalez-Espinosa, Signal transduction pathways activated by innate immunity in mast cells: translating sensing of changes into specific responses, Cells 9 (2020). http://10.3390/cells9112411.
[53] Y. Tao, Y.C. Chen, T. Lan, H. Qian, Y. Wang, L. Jiang, LPS-induced nuclear translocation of RhoA is dependent on NF-kappaB in the human lung cancer cell line A549, Oncol. Lett. 3 (2012) 1283–1287. http://10.3892/ol.2012.667.
[54] K. Atabai, M.A. Matthay, The pulmonary physician in critical care. 5: acute lung injury and the acute respiratory distress syndrome: definitions and epidemiology, Thorax 57 (2002) 452–458. http://10.1136/thorax.57.5.452.
[55] Y.F. Guo, N.N. Xu, W. Sun, Y. Zhao, C.Y. Li, M.Y. Guo, Luteolin reduces inflammation in Staphylococcus aureus-induced mastitis by inhibiting NF-kB activation and MMPs expression, Oncotarget 8 (2017) 28481–28493. http://10.18632/oncotarget.16092.
[56] K.F. Jiang, G. Zhao, G.Z. Deng, H.C. Wu, N.N. Yin, X.Y. Chen, et al., Polydatin ameliorates Staphylococcus aureus-induced mastitis in mice via inhibiting TLR2-mediated activation of the p38 MAPK/NF-kappaB pathway, Acta Pharmacol. Sin. 38 (2017) 211–222. http://10.1038/aps.2016.123.
[57] O. Bulgari, X. Dong, A.L. Roca, A.M. Caroli, J.J. Loor, Innate immune responses induced by lipopolysaccharide and lipoteichoic acid in primary goat mammary epithelial cells, J. Anim. Sci. Biotechnol. 8 (2017) 29. http://10.1186/s40104-017-0162-8.
[58] W. Wang, X. Hu, P. Shen, N. Zhang, Y. Fu, Sodium houttuyfonate inhibits LPS-induced inflammatory response via suppressing TLR4/NF-kB signaling pathway in bovine mammary epithelial cells, Microb. Pathog. 107 (2017) 12–16. http://10.1016/j.micpath.2017.03.011.
[59] L.A. O'Neill, A.G. Bowie, The family of five: TIR-domain-containing adaptors in Toll-like receptor signalling, Nat. Rev. Immunol. 7 (2007) 353–364. http://10.1038/nri2079.
[60] O. Takeuchi, S. Akira, Toll-like receptors; their physiological role and signal transduction system, Int. Immunopharm. 1 (2001) 625–635. http://10.1016/s1567-5769(01)00010-8.
[61] S. Giridharan, M. Srinivasan, Mechanisms of NF-kappaB p65 and strategies for therapeutic manipulation, J. Inflamm. Res. 11 (2018) 407–419. http://10.2147/JIR.S140188.
[62] M. Karin, Y. Yamamoto, Q.M. Wang, The IKK NF-kappa B system: a treasure trove for drug development, Nat. Rev. Drug Discov. 3 (2004) 17–26. http://10.1038/nrd1279.
[63] A. Oeckinghaus, S. Ghosh, The NF-kappaB family of transcription factors and its regulation, Cold Spring Harbor Perspect. Biol. 1 (2009) a000034. http://10.1101/cshperspect.a000034.
[64] F. Christian, E.L. Smith, R.J. Carmody, The regulation of NF-kappaB subunits by phosphorylation, Cells (2016) 5. http://10.3390/cells5010012.
[65] A. Borghi, L. Verstrepen, R. Beyaert, TRAF2 multitasking in TNF receptor-induced signaling to NF-kappaB, MAP kinases and cell death, Biochem. Pharmacol. 116 (2016) 1–10. http://10.1016/j.bcp.2016.03.009.
[66] S. Kaur, Y. Bansal, R. Kumar, G. Bansal, A panoramic review of IL-6: structure, pathophysiological roles and inhibitors, Bioorg. Med. Chem. 28 (2020), 115327. http://10.1016/j.bmc.2020.115327.
[67] A.A. Khan, M.A. Alsahli, A.H. Rahmani, Myeloperoxidase as an active disease biomarker: recent biochemical and pathological perspectives, Med. Sci. 6 (2018). http://10.3390/medsci6020033.
[68] R. Kralovics, A.S. Buser, S.-S. Teo, Coers Jr., A. Tichelli, A.P.C. van der Maas, et al., Comparison of molecular markers in a cohort of patients with chronic myeloproliferative disorders, Blood 102 (2003) 1869–1871. http://10.1182/blood-2003-03-0744.
[69] K. Göhring, J. Wolff, W. Doppl, K.L. Schmidt, K. Fenchel, H. Pralle, et al., Neutrophil CD177 (NB1 gp, HNA-2a) expression is increased in severe bacterial infections and polycythaemia vera, Br. J. Haematol. 126 (2004) 252–254. http://10.1111/j.1365-2141.2004.05027.x.